R. & M. No. 3795

PROCUREMENT EXECUTIVE, MINISTRY OF DEFENCE

AERONAUTICAL RESEARCH COUNCIL
REPORTS AND MEMORANDA

The Numerical Calculation of Subcritical Steady Potential Flow around an Unyawed Ellipsoid

By P. W. DUCK

Theoretical Aerodynamics Unit,
University of Southampton

LONDON: HER MAJESTY'S STATIONERY OFFICE

1977

£4 net

The Numerical Calculation of Subcritical Steady Potential Flow around an Unyawed Ellipsoid

By P. W. DUCK*

Theoretical Aerodynamics Unit,
University of Southampton

Reports and Memoranda No. 3795†
May, 1975

Summary

The problem of a subcritical, potential, steady, three-dimensional flow past an unyawed ellipsoid is considered, using ellipsoidal coordinates.

The full equations of motion and the exact body surface boundary condition are used throughout. Further, by means of a simple transformation the entire flow field is taken into the computation. A finite difference method, followed by an iterative process is used for the solution of the flow equations.

Mach number distributions are given for a number of examples, for the free-stream flow aligned along either the major axis, or the second major axis of the ellipsoid.

This work was done in association with Aerodynamics Department, R.A.E. under the link with the University of Southampton.

* Now at the Department of Mathematics, Imperial College, London.

† Replaces R.A.E. Technical Report 75041—A.R.C. 36 235

LIST OF CONTENTS

1. Introduction

The problem of calculating the exact (in the numerical sense) solution for two-dimensional, potential, subcritical flows past general shapes (with and without lift) has largely been solved, for some years now, primarily using the work of Sells[1].

Now, however, the recent development of powerful computing machines has introduced the possibility of calculating the flow around three-dimensional, wing- and body-like shapes.

Here we describe a numerical scheme that calculates the subcritical flow around an unyawed ellipsoid. The method is (numerically) exact, the full, non-linear equations of motion being used throughout, the entire flow field is taken into the computation, and the body surface boundary condition is satisfied as exactly as numerical differencing schemes will permit.

Throughout we work in ellipsoidal body coordinates. This enables us to satisfy the exact body surface boundary condition easily, and at the same time ensures a refined mesh distribution in regions in which the solution is changing rapidly. Further, by means of a simple transformation of one of these body coordinates, we are able to bring the entire physical flow field into a finite working field. The transformation also ensures that there is a certain amount of bunching of mesh points near the body, whilst further away the point distribution is sparser.

There are essentially two unknowns to the problem—the velocity potential and the speed of sound, which are connected by the Bernoulli energy conservation equation. The velocity potential has a singularity at infinity in the physical flow field, and this contribution is subtracted out of the calculation (being a known quantity) for numerical purposes.

Section 2 deals with the ellipsoidal body coordinate system, and the equations of motion in this coordinate system, together with the special mathematical treatment required along the singular lines encountered in these coordinates. Section 3 describes the numerical procedures required for computation, and the results are given in Section 4. There are three independent solutions to the problem of the unyawed ellipsoid, one for the freestream velocity aligned along each of the three body axes. Here we consider just two of the three cases, namely for the flow aligned along the two longest axes of the ellipsoid. The conclusions are given in Section 5.

2. The Ellipsoidal Coordinate System and the Equations of Motion

2.1. Ellipsoidal Coordinates

In this particular orthogonal, curvilinear coordinate system, the cartesian coordinates (x, y, z), using the well-known Jacobian elliptic functions are given in terms of the three ellipsoidal coordinates $\zeta^1, \zeta^2, \zeta^3$, by

$$x = [1+(\zeta^1)^2]^{\frac{1}{2}}\, dn\, \zeta^2\, \overline{sn}\, \zeta^3$$

$$y = [\sigma+(\zeta^1)^2]^{\frac{1}{2}}\, cn\, \zeta^2\, \overline{cn}\, \zeta^3$$

$$z = \zeta^1\, sn\, \zeta^2\, \overline{dn}\, \zeta^3$$

where for conciseness

$$sn\, \zeta^2 \equiv sn\, (\zeta^2, \sqrt{\sigma})$$

$$\overline{sn}\, \zeta^3 \equiv sn\, (\zeta^3, \sqrt{1-\sigma})$$

and similarly for the two other elliptic functions.

σ is a parameter that partly determines the shape of the ellipsoid, and for our purposes

$$0<\sigma<1.$$

In general

$$0 \leqslant \zeta^1 \leqslant \infty$$

$$-2K \leqslant \zeta^2 \leqslant 2K$$

$$-2K' \leqslant \zeta^3 \leqslant 2K',$$

where K and K' are the complete elliptic integral and the complementary complete integral respectively, of the first kind, viz.

$$K = \int_0^{\pi/2} \frac{d\theta}{[1-\sigma \sin^2\theta]^{\frac{1}{2}}}$$

$$K' = \int_0^{\pi/2} \frac{d\theta}{[1-(1-\sigma)\sin^2\theta]^{\frac{1}{2}}}.$$

The surfaces $\zeta^1, \zeta^2, \zeta^3$ = constant are an ellipsoid, a hyperboloid of one sheet, and a hyperboloid of two sheets respectively.

The equations defining these surfaces are

$$\frac{x^2}{1+(\zeta^1)^2}+\frac{y^2}{\sigma+(\zeta^1)^2}+\frac{z^2}{(\zeta^1)^2}=1$$

$$\frac{x^2}{dn^2\,\zeta^2}+\frac{y^2}{\sigma\, cn^2\,\zeta^2}-\frac{z^2}{\sigma\, sn^2\,\zeta^2}=1$$

$$\frac{x^2}{(1-\sigma)\,\overline{sn}^2\,\zeta^3}-\frac{y^2}{(1-\sigma)\,\overline{cn}^2\,\zeta^3}-\frac{z^2}{\overline{dn}^2\,\zeta^3}=1.$$

For our purposes we set $\zeta^1 = \zeta_0^1$ = constant to complete the definition of the ellipsoid.

It is convenient to introduce the curvilinear metrics of the system. For a general orthogonal system the three curvilinear metrics A_i $(i = 1, 2, 3)$ are given by

$$A_i^2 = \left(\frac{\partial x}{\partial \zeta^i}\right)^2 + \left(\frac{\partial y}{\partial \zeta^i}\right)^2 + \left(\frac{\partial z}{\partial \zeta^i}\right)^2 \qquad i = 1, 2, 3.$$

Then for the ellipsoidal coordinate system

$$A_1 = B_2 B_3 B^*$$

$$A_2 = B_1 B_3$$

$$A_3 = B_1 B_2$$

where

$$B^* = [1+(\zeta^1)^2]^{-\frac{1}{2}}[\sigma+(\zeta^1)^2]^{-\frac{1}{2}}$$

$$B_1 = [\sigma\, cn^2\,\zeta^2 + (1-\sigma)\,\overline{cn}^2\,\zeta^3]^{\frac{1}{2}}$$

$$B_2 = [\overline{dn}^2\,\zeta^3 + (\zeta^1)^2]^{\frac{1}{2}}$$

$$B_3 = [\sigma\, sn^2\,\zeta^2 + (\zeta^1)^2]^{\frac{1}{2}}.$$

For a more detailed examination of general coordinate systems, see Mangler and Murray[2].

2.2 Equations of Motion

The continuity equation in a general coordinate system may be written in the form

$$\frac{1}{J}\frac{\partial}{\partial \zeta^i}(Jg^{ij}V_j) - \frac{g^{ij}V_j}{a^2} q \frac{\partial q}{\partial \zeta^i} = 0 \tag{1}$$

where V_j are the covariant velocity components, J is the Jacobian of the system, and g^{ij} are the contravariant metric tensors of order two.

The speed of sound a, is obtained from the Bernoulli energy equation, *viz.*

$$\frac{a^2}{\gamma-1}+\frac{1}{2}q^2 = \text{constant}$$

where q is the fluid speed, i.e.

$$q^2 = g^{ij} V_i V_j.$$

Remembering that for an orthogonal system

$$g_{ii} = (A_i)^2 \qquad \text{(no summation)}$$
$$g_{ij} = 0 \qquad (i \neq j).$$

Then

$$J = \sqrt{g_{11} g_{22} g_{33}}$$
$$= A_1 A_2 A_3.$$

Further since the flow is irrotational, there exists a velocity potential Φ, where

$$V_i = \frac{\partial \Phi}{\partial \zeta^i} \qquad i = 1, 2, 3$$

and equation (1) may be written in the form

$$\frac{1}{A_1 A_2 A_3} \frac{\partial}{\partial \zeta^i} \left[A_1 A_2 A_3 (A^i)^2 \frac{\partial \Phi}{\partial \zeta^i} \right] - \frac{(A^i)^2}{2a^2} \frac{\partial (q^2)}{\partial \zeta^i} \frac{\partial \Phi}{\partial \zeta^i} = 0 \tag{2}$$

where $A^i = 1/A_i$ for orthogonal systems.

If we now consider the special case of the ellipsoidal coordinate system, equation (2) becomes

$$\begin{aligned}
&\frac{1}{B_2^2 B_3^2 B^{*2}} \left(1 - \frac{\Phi_1^2}{B_2^2 B_3^2 B^{*2} a^2} \right) \Phi_{11} - \frac{2\Phi_1 \Phi_2}{B_1^2 B_2^2 B_3^4 B^{*2} a^2} \Phi_{12} + \frac{1}{B_1^2 B_3^2} \left(1 - \frac{\Phi_2^2}{B_1^2 B_3^2 a^2} \right) \Phi_{22} \\
&- \frac{2\Phi_1 \Phi_3}{B_1^2 B_2^4 B_3^2 a^2} \Phi_{13} - \frac{2\Phi_2 \Phi_3}{B_1^4 B_2^2 B_3^2 a^2} \Phi_{23} + \frac{1}{B_1^2 B_2^2} \left(1 - \frac{\Phi_3^2}{B_1^2 B_2^2 a^2} \right) \Phi_{33} \\
&+ \frac{\Phi_1}{B_2^2 B_3^2 B^*} \frac{\partial}{\partial \zeta^1} \left(\frac{1}{B^*} \right) + \frac{V^i}{2 B_2^2 B_3^2 B^{*2}} \left(\frac{\Phi_1}{B_2 B_3 B^* a} \right)^2 \frac{\partial}{\partial \zeta^i} (B_2^2 B_3^2 B^{*2}) \\
&+ \frac{V^i}{2 B_1^2 B_3^2} \left(\frac{\Phi_2}{B_1 B_3 a} \right)^2 \frac{\partial}{\partial \zeta^i} (B_1^2 B_3^2) + \frac{V^i}{2 B_1^2 B_2^2} \left(\frac{\Phi_3}{B_1 B_2 a} \right)^2 \frac{\partial}{\partial \zeta^i} (B_1^2 B_2^2) = 0
\end{aligned} \tag{3}$$

where

$$\Phi_i \equiv \frac{\theta \Phi}{\partial \zeta^i} \equiv \Phi_{,i}$$

$$\Phi_{ij} \equiv \frac{\partial^2 \Phi}{\partial \zeta^i \, \partial \zeta^j} \equiv \Phi_{,ij}$$

and

$$V^i = \frac{V_i}{(A_i)^2} = \frac{\Phi_i}{(A_i)^2} \text{ (no summation).}$$

We now find it convenient to introduce the transformation

$$\bar{\zeta}^1 = \int_0^{\zeta^1} B^* \, d\zeta^1$$
$$= \int_0^{\zeta^1} \frac{d\zeta^1}{(1 + (\zeta^1)^2)^{\frac{1}{2}} (\sigma + (\zeta^1)^2)^{\frac{1}{2}}}$$

i.e.

$$\zeta^1 = \sqrt{\sigma}\,\overline{tn}\,\bar{\zeta}^1$$

where

$$\overline{tn}\,\bar{\zeta}^1 \equiv tn\,(\bar{\zeta}^1, \sqrt{1-\sigma})$$

$$\equiv \overline{sn}\,\bar{\zeta}^1 / \overline{cn}\,\bar{\zeta}^1$$

and for our purposes

$$\bar{\zeta}_0^1 \leqslant \bar{\zeta}^1 \leqslant K'$$

as

$$\zeta_0^1 \leqslant \zeta^1 \leqslant \infty.$$

As well as simplifying slightly equation (3), this transformation brings the entire physical field into a finite working field, and so there is no need to impose arbitrary outer boundaries in order to obtain a finite range for the computation. This transformation will also ensure a denser distribution of mesh points near the body in the flow field, and fewer points as infinity is approached in the physical field, when the finite difference approximation is made.

After some algebra, the continuity equation (3) becomes

$$\begin{aligned}
&\frac{1}{B_2^2B_3^2}\left(1-\frac{\Phi_I^2}{B_2^2B_3^2a^2}\right)\Phi_{II} - \frac{2\Phi_I\Phi_2}{B_1^2B_2^2B_3^4a^2}\Phi_{I2} + \frac{1}{B_1^2B_3^2}\left(1-\frac{\Phi_2^2}{B_1^2B_3^2a^2}\right)\Phi_{22} - \frac{2\Phi_I\Phi_3}{B_1^2B_2^4B_3^2}\Phi_{13} \\
&\qquad - \frac{2\Phi_2\Phi_3}{B_1^4B_2^2B_3^2a^2}\Phi_{23} + \frac{1}{B_1^2B_2^2}\left(1-\frac{\Phi_3^2}{B_1^2B_2^2a^2}\right)\Phi_{33} \\
&+ \frac{\Phi_I^2}{2B_2^4B_3^4a^2}\left[\frac{\Phi_I}{B_2^2B_3^2}\frac{\partial}{\partial\bar{\zeta}^1}(B_2^2B_3^2) + \frac{B_2^2}{B_1^2B_3^2}\Phi_2\frac{\partial}{\partial\zeta^2}(B_3^2) + \frac{B_3^2}{B_1^2B_2^2}\Phi_3\frac{\partial}{\partial\zeta^3}(B_2^2)\right] \\
&+ \frac{\Phi_2^2}{2B_1^4B_3^4a^2}\left[\frac{B_1^2}{B_2^2B_3^2}\Phi_I\frac{\partial}{\partial\bar{\zeta}^1}(B_3^2) + \frac{\Phi_2}{B_1^2B_3^2}\frac{\partial}{\partial\zeta^2}(B_1^2B_3^2) + \frac{B_3^2}{B_1^2B_2^2}\Phi_3\frac{\partial}{\partial\zeta^3}(B_1^2)\right] \\
&+ \frac{\Phi_3^2}{2B_1^4B_2^4a^2}\left[\frac{B_1^2}{B_2^2B_3^2}\Phi_I\frac{\partial}{\partial\bar{\zeta}^1}(B_2^2) + \frac{B_2^2}{B_1^2B_3^2}\Phi_2\frac{\partial}{\partial\zeta^2}(B_1^2) + \frac{\Phi_3}{B_1^2B_2^2}\frac{\partial}{\partial\zeta^3}(B_1^2B_2^2)\right] = 0
\end{aligned} \tag{4}$$

where

$$\Phi_I \equiv \frac{\partial\Phi}{\partial\bar{\zeta}^1}$$

$$\Phi_{II} \equiv \frac{\partial^2\Phi}{\partial(\bar{\zeta}^1)^2}$$

$$\Phi_{Ii} \equiv \frac{\partial^2\Phi}{\partial\bar{\zeta}^1\,\partial\zeta^i}.$$

The boundary condition on the surface of the body ($\bar{\zeta}^1 = \bar{\zeta}_0^1$, $\zeta^1 = \zeta_0^1 = \sqrt{\sigma}\,\overline{tn}\,\bar{\zeta}_0^1$ is

$$\Phi_I = 0 \tag{5}$$

whilst as $\bar{\zeta}_0^1 \to K'$, $\Phi \to \Phi_\infty$ where Φ_∞ is the freestream (undisturbed) potential.

2.3. Singular Lines of Transformation

We find that there are singular lines, along which the Jacobian of the transformation vanishes. This occurs if any of the $B_i = 0$ (which implies that $A_{i-1}, A_{i+1} = 0$).

Since we are dealing with a non-zero ellipsoid, then $\zeta^1 \geq \zeta_0^1 > 0$ and consequently B_2 and B_3 do not vanish in the flow field.

However $B_1 = 0$ along the lines $\zeta^2 = \pm K$, $\zeta^3 = \pm K'$ which correspond in the cartesian system to the hyperbolae

$$\frac{x^2}{1-\sigma} - \frac{z^2}{\sigma} = 1, \qquad y = 0.$$

Along these hyperbolae, A_2 and A_3 vanish and special attention is required in order to establish the equation of motion and the fluid speed q.

In general

$$q^2 = V_i V^i = g^{ij} V_i V_j$$
$$= \frac{V_1^2}{A_1^2} + \frac{V_2^2}{A_2^2} + \frac{V_3^2}{A_3^2}.$$

For ellipsoidal coordinates

$$q^2 = \frac{V_I^2}{B_2^2 B_3^2} + \frac{V_2^2}{B_1^2 B_3^2} + \frac{V_3^2}{B_1^2 B_2^2}. \tag{6}$$

We now examine the behaviour of the above expression along these singular lines, where $B_1 = 0$ and V_2, $V_3 = 0$ (this follows immediately from the symmetry of the problem).

Now if $u_i = \Phi_i/(B_{i-1}B_{i+1})$, $u_I = \Phi_I/(B_2 B_3)$ then

$$q^2 = u_I^2 + u_2^2 + u_3^2,$$

where u_I^2 presents no problem.

In order to calculate the sum of the other two velocity components, we consider a second orthogonal coordinate system $(\zeta^1, \eta^2, \eta^3)$, with origin at the point $(0, K, K')$ in the original $(\zeta^1, \zeta^2, \zeta^3)$ coordinate system. ζ^1 remains unchanged but η^2 and η^3 are inclined at an angle ψ to ζ^2 and ζ^3 respectively as shown in Fig. 1.

Then

$$\eta^2 = (\zeta^2 - K)\cos\psi - (\zeta^3 - K')\sin\psi$$

$$\eta^3 = (\zeta^2 - K)\sin\psi + (\zeta^3 - K')\cos\psi.$$

Now

$$u_2^2 + u_3^2 = \frac{\Phi_2^2}{B_1^2 B_3^2} + \frac{\Phi_3^2}{B_1^2 B_2^2}$$
$$= \frac{[\Phi_{\eta^2}\cos\psi + \Phi_{\eta^3}\sin\psi]^2}{B_1^2 B_3^2} + \frac{[\Phi_{\eta^3}\cos\psi - \Phi_{\eta^2}\sin\psi]^2}{B_1^2 B_2^2}. \tag{7}$$

Applying L'Hôpital's rule twice to equation (7) we obtain

$$[u_2^2 + u_3^2]_{\substack{\eta^2 \to 0 \\ \eta^3 = 0}} = \frac{2[(\Phi_{\eta^3\eta^2})^2 + (\Phi_{\eta^2\eta^2})^2]}{(B_1^2)_{\eta^2\eta^2}[\sigma + (\zeta^1)^2]}. \tag{8}$$

Alternatively

$$[u_2^2 + u_3^2]_{\substack{\eta^3 \to 0 \\ \eta^2 = 0}} = \frac{2[(\Phi_{\eta^3\eta^3})^2 + (\Phi_{\eta^2\eta^3})^2]}{(B_1^2)_{\eta^2\eta^3}[\sigma + (\zeta^1)^2]} \tag{9}$$

where

$$\Phi_{\eta^i} = \frac{\partial \Phi}{\partial \eta^i}$$

$$\Phi_{\eta^i \eta^i} = \frac{\partial^2 \Phi}{\partial (\eta^i)^2}$$

$$\Phi_{\eta^i \eta^j} = \frac{\partial^2 \Phi}{\partial \eta^i \, \partial \eta^j}$$

$$(B_1^2)_{\eta^i \eta^i} = \frac{\partial^2}{\partial (\eta^i)^2}(B_1^2).$$

Now

$$[(B_1^2)_{\eta^2 \eta^2}]_{\substack{\eta^2 = 0 \\ \eta^3 = 0}} = [(B_1^2)_{\eta^3 \eta^3}]_{\substack{\eta^2 = 0 \\ \eta^3 = 0}}$$

and because equations (8) and (9) must be equivalent (the flow speed must be independent of the direction of approach)

$$\Phi_{\eta^3 \eta^3} \pm \Phi_{\eta^2 \eta^2} = 0.$$

Taking the positive sign we obtain

$$\Phi_{22} + \Phi_{33} = 0. \tag{10}$$

Taking the negative sign we obtain

$$\Phi_{22} - \Phi_{33} + 2 \tan 2\psi \Phi_{23} = 0. \tag{11}$$

However this latter equation implies that the equation of motion along the singular lines is dependent on the direction of approach of the lines, and so must be neglected in favour of equation (10).

Consequently in order to calculate the flow speed (and hence Mach number) along the singular lines we use

$$u_2^2 + u_3^2 = \frac{(\Phi_{23})^2 + (\Phi_{22})^2}{\sigma(1-\sigma)[\sigma + (\zeta^1)^2]}$$

$$= \frac{(\Phi_{23})^2 + (\Phi_{33})^2}{\sigma(1-\sigma)[\sigma + (\zeta^1)^2]}.$$

3. Numerical Techniques

In its present form, equation (4) is unsuitable for numerical treatment. Firstly negative powers of B_1 occur, and as discussed previously, $B_1 = 0$ along the lines $\zeta^2 = \pm K$, $\zeta^3 = \pm K'$. However we have shown in the previous section that along these singular lines, the continuity equation reduces to (10). Thus for mesh points situated along these lines, (10) must be used in place of (4).

Secondly Φ has a singularity at $\zeta^1 = K'$ ($\zeta^1 = \infty$). However this singular contribution to Φ is known, and may be subtracted out of the potential, leaving a perturbation potential ϕ which is finite everywhere, i.e.

$$\Phi = \Phi_s + \phi.$$

This singularity arises from the freestream flow. Thus we can set

$$\Phi_s = \Phi_\infty. \tag{12}$$

Alternatively since we know the exact incompressible solution Φ^* (*see* Appendix A), then we can put

$$\Phi_s = \Phi_\infty + \Phi^*. \tag{13}$$

In both cases, the partial differential equation in ϕ is approximated by a (central) finite difference equation, where the derivatives at the point $(\bar{\zeta}_0^1 + l\delta_1, m\delta_2, n\delta_3)$ are given by

$$(\phi_I)_{l,m,n} = \frac{1}{2\delta_1}(\phi_{l+1,m,n} - \phi_{l-1,m,n}) + O(\delta_1^2)$$

$$(\phi_{II})_{l,m,n} = \frac{1}{\delta_1^2}(\phi_{l+1,m,n} - 2\phi_{l,m,n} + \phi_{l-1,m,n}) + O(\delta_1^2)$$

$$(\phi_{I2})_{l,m,n} = \frac{1}{4\delta_1\delta_2}(\phi_{l+1,m+1,n} - \phi_{l+1,n-1,n} - \phi_{l-1,n+1,n} + \phi_{l-1,n-1,n}) + O(\delta_1^2 + \delta_2^2)$$

with similar expressions for the other derivatives of ϕ. δ_1, δ_2 and δ_3 are the cell dimensions in the $\bar{\zeta}^1$, ζ^2 and ζ^3 directions respectively. Derivatives of Φ_s may be calculated analytically.

The difference equation, at the point $(\bar{\zeta}_0^1 + l\delta_1, m\delta_2, n\delta_3)$ may be written in the form

$$d_n\phi_{l,m,n-1} + c_n\phi_{l,m,n} + b_n\phi_{l,m,n+1} = a_n \tag{14}$$

where a_n contains the contributions in the difference equation from the other 12 neighbouring mesh points. Details of the a_n, b_n, c_n and d_n are given in Appendix B. Similar expressions to (14) may be written for the l- or m- ($\bar{\zeta}^1$ or ζ^2) directions.

It can be shown (Varga[3]) that if a matrix is diagonally dominant (the absolute value of the diagonal element is greater than the sum of the absolute values of the off-diagonal elements) then the point Gauss–Seidel method is convergent. Further if this method is convergent, then for block tridiagonal matrices, such as is represented by a set of equations (14), with l, m fixed, n varying, it is quicker to solve for blocks rather than individual points during the iterative process. For this purpose, a variant of Choleski's method was used (*see*, for example, Hartree[4]) in which the submatrix is first factorised into upper and lower matrices for inversion.

Again, a similar process may be applied for solution along lines of l, n fixed and m varying, or m, n fixed and l varying.

In order to start the iterative process, the initial guess used was the exact, incompressible perturbation solution Φ^*, i.e. if

$$\Phi_s = \Phi_\infty$$

then

$$\phi = \Phi^*$$

whilst if

$$\Phi_s = \Phi_\infty + \Phi^*$$

then

$$\phi = 0.$$

For the purpose of the computation, symmetry was invoked fully in order to reduce demands in both computer storage and time.

Since the velocity potential was the flow field quantity stored throughout the computation, the convergence criterion adopted was that the iteration process was stopped when the maximum change in potential encountered anywhere within the flow field was less than 1×10^{-6} during one iteration. This corresponds to a change in local Mach number of about 1×10^{-5}.

In order to transform the final iterated solution into cartesian coordinates, two linear interpolation routines were used. One gave the Mach number distribution on the surface of the ellipsoid, whilst the other produced lines along which the Mach number remained constant.

A number of runs was carried out using different mesh sizes in order to test the effect of mesh size on two of the calculations and the results are shown in Tables 1 and 2. In the first example, for which the freestream is

aligned along the major axis of the body (Table 1), the solution appears fairly insensitive to changes of cell dimensions in any of the three body coordinates. In the other example (Table 2) for which the freestream is aligned with the second major axis, the calculation appears more sensitive to changes in mesh size, particularly in the region of the stagnation point. The calculation in general appears especially sensitive to changes in the number of points taken in the coordinate perpendicular to the body surface. It should be noted that the discrepancy in the region of the stagnation point in the cases for which the number of points in the ζ^2 direction was decreased, is largely due to the linear interpolation routine, because of the rapid rise in Mach number in this direction in this region. Examination of the uninterpolated results shows closer agreement. The results seem to indicate convergence of local Mach number with decreasing mesh size.

Generally the numerical system was well behaved, and in order to increase the rate of convergence, over-relaxation was applied to the velocity potential. If $\phi^{(N)}_{l,m,n}$ denotes the value of $\phi_{l,m,n}$ found by block inversion during the Nth iteration cycle, and $\phi^{(N-1)}_{l,m,n}$ the previous value, then the new value is

$$\phi^{(N)}_{l,m,n} = \omega_b \phi^{(N)}_{l,m,n} + (1-\omega)\phi^{(N-1)}_{l,m,n}$$

where ω is the relaxation parameter.

Usually relaxation parameters of 1·8 to 1·9 gave adequate stability and rate of convergence. Solving along lines of varying ζ^2 generally gave the best stability and rate of convergence. For a typical calculation, solving along varying ζ^2 lines, 20–60 iterations were required to satisfy the convergence criterion. Solutions obtained along different coordinate directions were numerically identical.

Further setting $\Phi_s = \Phi_\infty + \Phi^*$, instead of $\Phi_s = \Phi_\infty$, had little effect on the numerical system. Local Mach numbers differed by no more than 1×10^{-4}.

4. Results

Tables 3–8 and Figs. 3–6 and 8 and 9 show the Mach number distribution on the surface of a number of ellipsoids at various Mach numbers. Figs. 2 and 7 show the lines on the body surface along which the Mach number is constant.

For the cases in which $\Phi_\infty = x$, the constant speed of flow along the second major axis of the ellipsoid, present in the incompressible solution, is still present, to within 2×10^{-4} in Mach number.

For the examples for which $\Phi_\infty = y$, the Mach number is approximately constant along the major axes, although it appears to increase as the tips are approached, the variation in the example in Table 4 being about 0·6 per cent. Further this effect was seen to increase with an increase in aspect ratio and also with an increase in freestream Mach number.

Fig. 10 shows the variation of normalised flow speed, at the point on the surface given in cartesian coordinates by $(0, 0, \zeta^1_0)$ with the reciprocal of aspect ratio (aspect ratio $= (4/\pi)[1+(\zeta^1_0)^2]^{\frac{1}{2}}[\sigma+(\zeta^1_0)^2]^{-\frac{1}{2}}$). The ellipsoids all have thickness/chord ratios of 10 per cent. For comparison the exact incompressible result is shown, as are three theoretical values obtained for a 10 per cent, two-dimensional, elliptic section. One value was obtained by Rasmussen and Heys[5] using a variational method, a second by Clapworthy[6] solving for potential, and the third by the author using Sells' method[1]. The results of the latter two calculations are almost identical, giving a value of $q/q_\infty = 1{\cdot}200$. As expected the present three-dimensional calculations approach the two-dimensional values as the aspect ratio is increased, to within the numerical accuracy of the four sets of calculations.

5. Conclusions

We have shown that a finite difference approximation to the full equation of motion, expressed in ellipsoidal coordinates, can produce a satisfactory numerical solution for the three-dimensional flow around an unyawed ellipsoid.

The main advantages of using this body coordinate system are, a simplification of the treatment of the body surface boundary condition, and a refined mesh distribution (in the physical flow field) where the solution is changing rapidly. The only real problem, namely the mathematical treatment along the singular lines along which the Jacobian of the transformation vanishes, appears to present no serious difficulties.

The numerical scheme is generally well behaved, with usually just 20 to 60 iterations required for maximum changes in velocity potential of less than 1×10^{-6} per iteration, for a $20 \times 21 \times 20$ mesh. This corresponds to changes of local Mach number of about 1×10^{-5}. Computations usually take no more than 70 seconds on a CDC 7600.

An extension of the present work is planned to ellipsoids in mixed flows. This will require the application of retarded difference schemes (Murman and Cole[7]) in the supersonic regions, along rotated coordinate axes (Jameson[8]). Further the fore and aft symmetry invoked in the present subcritical case will be lost, as a result of the appearance of shock waves in the flow.

Acknowledgments

This work was carried out at the Theoretical Aerodynamics Research Unit, University of Southampton. The author is indebted to Professor K. W. Mangler for many helpful discussions and comments. The financial assistance of the SRC is gratefully acknowledged. The computations were carried out at the Computing Centre, University of Southampton, using the link to the U.L.C.C. C.D.C. 7600.

LIST OF SYMBOLS

a	Speed of sound
a_n, b_n, c_n, d_n	Coefficients in matrix equation
A_i	Curvilinear metrics
A^i	$1/A_i$ (for orthogonal systems)
B_i, B^*	Magnitudes relating to the A_i
C_1, C_2	Constants of integration (Appendix B)
$E(\theta, \sqrt{1-\sigma})$	Incomplete elliptic integral of the second kind, modulus $\sqrt{1-\sigma}$, amplitude θ
$f(\zeta^1)$	See (B-2)
$F(\theta, \sqrt{1-\sigma})$	Incomplete elliptic integral of the first kind, modulus $\sqrt{1-\sigma}$, amplitude θ
g^{ij}	Contra-variant metric tensor of order 2
g_{ij}	Co-variant metric tensor of order 2
J	Jacobian of transformation
$K(\sqrt{\sigma}$	Complete elliptic integral of first kind
$K'(\sqrt{\sigma})$	$K(\sqrt{1-\sigma})$ complementary complete elliptic integral of the first kind
l, m, n	Indices identifying points in field
M	Mach number
q	Fluid speed
u_i	$\Phi_i/(B_{i-1}B_{i+1})$
V_j	$\partial\Phi/\partial\zeta^i$
V^i	$g^{ij}V_j$
x, y, z	Cartesian coordinates
$\bar{x}, \bar{y}$	Sectional cartesian coordinates
γ	Ratio of specific heats
δ_i	Mesh size in ith coordinate direction
ζ^i	ith coordinate
$\bar{\zeta}^1$	Coordinate in (transformed) $\bar{\zeta}^1$ direction
η^i	Rotated coordinate
θ	Amplitude of elliptic integrals
σ	Parameter partly determining dimensions of ellipsoid
ϕ	Unknown contribution to potential
Φ	Total potential
Φ_i	$\partial\Phi/\partial\zeta^i$
Φ_{ij}	$\partial^2\Phi/\partial(\zeta^i)\,\partial(\zeta^j)$
Φ_I	$\partial\Phi/\partial\bar{\zeta}^1$
Φ_{Ii}	$\partial^2\Phi/\partial\bar{\zeta}^1\,\partial\zeta^i$

Φ_{η^i}	$\partial\Phi/\partial\eta^i$
$\Phi_{\eta^i\eta^j}$	$\partial^2\Phi/\partial\eta^i\,\partial\eta^j$
Φ^*	Incompressible (perturbation) potential
ψ	Angle between $\zeta^2(\zeta^3)$ and $\eta^2(\eta^3)$
ω	Relaxation parameter

Subscripts

b	Value obtained directly from block inversion
ijk	Indices running from 1 to 3
l, m, n	Conditions at point $(\bar{\zeta}_0^1 + l\delta_1, m\delta_2, n\delta_3)$
M	Maximum value
0	Conditions on body surface
s	Known contribution (contains singularity)
∞	Freestream conditions

Superscripts

ijk	Indices running from 1 to 3
(N)	Value from Nth iteration

REFERENCES

1 C. C. L. Sells ..... Plane subcritical flow past a lifting aerofoil. *Proc. Roy. Soc.*, A308, pp. 377–401 1968

2 K. W. Mangler and J. C. Murray ..... Systems of coordinates suitable for the numerical calculation of three-dimensional flow fields. A.R.C., C.P. No. 1325, 1973.

3 R. S. Varga ..... *Matrix iterative analysis.* Prentice-Hall, N.J., 1962

4 D. R. Hartree ..... *Numerical analysis.* O.U.P., 1964

5 H. Rasmussen and N. Heys ..... Application of a variational method in plane compressible flow calculation. *J. Inst. Maths Applics.* 13, pp. 47–61, 1974

6 G. J. Clapworthy ..... Private communication.

7 E. Murman and J. D. Cole ..... Calculation of plane steady transonic flow. *AIAA Journal*, Vol. 9, pp. 114–121, 1971

8 A. Jameson ..... Iterative solution of transonic flows over airfoils and wings, including flows at Mach 1. *Communs. pure appl. Math.*, Vol. 27, pp. 283–309, 1974

APPENDIX A

Exact Incompressible Solution

The continuity equation, in ellipsoidal coordinates, for incompressible flow reduces to

$$\frac{B_1^2}{B^*}\frac{\partial}{\partial\zeta^1}\left(\frac{1}{B^*}\frac{\partial\Phi}{\partial\zeta^1}\right)+B_2^2\frac{\partial^2\Phi}{\partial(\zeta^2)^2}+B_3^2\frac{\partial^2\Phi}{\partial(\zeta^3)^2}=0. \tag{A-1}$$

Consider first the case for which the freestream velocity potential is given by

$$\Phi_\infty = x.$$

Then since $\Phi = x$ will be a solution of (A-1) we try for another solution, of the form

$$\Phi = xf(\zeta^1) \tag{A-2}$$

remembering $x = [1+(\zeta^1)^2]^{\frac{1}{2}}\, dn\,\zeta^2\, \overline{sn}\,\zeta^3$.

Having substituted (A-2) into (A-1), we obtain, after some algebra

$$f''+\left(\frac{3\zeta^1}{1+(\zeta^1)^2}+\frac{\zeta^1}{\sigma+(\zeta^1)^2}\right)f'=0.$$

The solution for this first order ordinary differential equation in f' may be written in the form

$$f(\zeta^1)=C_1\int_{\zeta'}^{\infty}\frac{d\zeta^1}{[1+(\zeta^1)^2)^{3/2}[\alpha+(\zeta^1)^2]^{\frac{1}{2}}} \tag{A-3}$$

where the limits of integration are chosen for convenience, so that

$$f(\zeta^1)\to 0 \quad \text{as} \quad \zeta^1\to\infty$$

whilst C_1 must be chosen such that the surface boundary condition $(\partial\Phi/\partial\zeta^1)_{\zeta^1=\zeta_0^1}=0$ is satisfied.

(A-3) may be integrated to give

$$f(\zeta^1)=\frac{C_1}{1-\sigma}[F(\theta,\sqrt{1-\sigma})-E(\theta,\sqrt{1-\sigma})]$$

where $F(\theta,\sqrt{1-\sigma})$, and $E(\theta,\sqrt{1-\sigma})$ are the incomplete elliptic integrals of the first and second kind respectively, with modulus $\sqrt{1-\sigma}$ and argument θ where

$$\theta=\tan^{-1}\frac{1}{\zeta^1}.$$

The surface boundary condition gives

$$C_1=\frac{(1-\sigma)\zeta_0^1\sqrt{(1+(\zeta_0^1)^2)(\sigma+(\zeta_0^1)^2)}}{[(1-\sigma)-\zeta_0^1\sqrt{(1+(\zeta_0^1)^2)(\sigma+(\zeta_0^1)^2)}(F_0-E_0)]}$$

where

$$\left.\begin{aligned} F_0&=F(\theta_0,\sqrt{1-\sigma})\\ E_0&=E(\theta_0,\sqrt{1-\sigma})\\ \theta_0&=\tan^{-1}\frac{1}{\zeta_0^1}\end{aligned}\right\}. \tag{A-4}$$

A similar analysis for $\Phi_\infty = y$, assuming a perturbation solution of the form

$$\Phi = f(\zeta^1)y$$

yields

$$f(\zeta^1) = \frac{C_2}{\sigma(1-\sigma)}\left[E(\theta,\sqrt{1-\sigma}) - \sigma F(\theta,\sqrt{1-\sigma}) - \frac{(1-\sigma)\zeta^1}{\sqrt{(1+(\zeta^1)^2)(\sigma+(\zeta^1)^2)}}\right]$$

where

$$C_2 = \frac{\sigma(1-\sigma)\zeta_0^1\sqrt{(1+(\zeta_0^1)^2)(\sigma+(\zeta_0^1)^2)}}{\{\sigma(1-\sigma) - [(E_0-\sigma F_2)\zeta_0^1\sqrt{(1+(\zeta_0^1)^2)(\sigma+(\zeta_0^1)^2)} - (\zeta_0^1)^2(1-\sigma)]\}}$$

where F_0 and E_0 are as defined in (A-4).

APPENDIX B

Details of Difference Equation

Here we assume throughout that we are solving along lines of varying ζ^3, and constant $\bar{\zeta}^1$ and ζ^2, but similar expressions may be obtained for solutions in the two other coordinate directions. Then, we can write the difference equations in the form

$$d_n\,{}_b\phi^{(N)}_{l,m,n-1} + c_n\,{}_b\phi^{(N)}_{l,m,n} + b_n\,{}_b\phi^{(N)}_{l,m,n+1} = a_n \tag{B-1}$$

subscript b's denoting values obtained directly from the solution of (B-1), i.e. with no relaxation parameter applied. For the Nth iteration, away from the singular lines, we have

$$d_n = \frac{1}{B_1^2B_2^2\delta_3^2}\left(1-\frac{\Phi_3^2}{B_1^2B_2^2a^2}\right) - \frac{\Phi_I^2}{4B_1^2B_2^6B_3^2a^2\delta_3}\frac{\partial}{\partial\zeta^3}(B_2^2) - \frac{\Phi_2^2}{4B_1^6B_2^2B_3^2a^2\delta_3}\frac{\partial}{\partial\zeta^3}(B_1^2) - \frac{\Phi_3^2}{4B_1^6B_2^6a^2\delta_3}\frac{\partial}{\partial\zeta^3}(B_1^2B_2^2)$$

$$b_n = \frac{1}{B_1^2B_2^2\delta_3^2}\left(1-\frac{\Phi_3^2}{B_1^2B_2^2a^2}\right) + \frac{\Phi_I^2}{4B_1^2B_2^6B_3^2a^2\delta_3}\frac{\partial}{\partial\zeta^3}(B_2^2) + \frac{\Phi_2^2}{4B_1^6B_2^2B_3^2a^2\delta_3}\frac{\partial}{\partial\zeta^3}(B_1^2) + \frac{\Phi_3^2}{4B_1^6B_2^6a^2\delta_3}\frac{\partial}{\partial\zeta^3}(B_1^2B_2^2)$$

$$c_n = -2\left\{\frac{1}{B_2^2B_3^2\delta_1^2}\left(1-\frac{\Phi_I^2}{B_2^2B_3^2a^2}\right) + \frac{1}{B_1^2B_3{}^2\delta_2^2}\left(1+\frac{\Phi_2^2}{B_1^2B_3^2a^2}\right) + \frac{1}{B_1^2B_3^2\delta_3^2}\left(1-\frac{\Phi_3^2}{B_1^2B_2^2a^2}\right)\right\}$$

$$\begin{aligned}
a_n = &-\frac{1}{B_2^2B_3^2}\left(1-\frac{\Phi_I^2}{B_1^2B_3^2a^2}\right)\left(\Phi_{s_{II}} + \frac{\phi_{l+1,m,n}+\phi_{l-1,m,n}}{\delta_1^2}\right)\\
&-\frac{1}{B_1^2B_3^2}\left(1-\frac{\Phi_2^2}{B_1^2B_3^2a^2}\right)\left(\Phi_{s_{22}} + \frac{\phi_{l,m+1,n}+\phi_{l,m-1,n}}{\delta_2^2}\right)\\
&-\frac{1}{B_1^2B_2^2}\left(1-\frac{\Phi_3^2}{B_1^2B_2^2a^2}\right)\Phi_{s_{33}} + \frac{2\Phi_I\Phi_2}{B_1^2B_2^2B_3^4a^2}\Phi_{s_{I2}} + \frac{2\Phi_1\Phi_3}{B_1^2B_2^4B_3^2a^2}\Phi_{I3} + \frac{2\Phi_2\Phi_3}{B_1^4B_2^2B_3^2a^2}\Phi_{23}\\
&-\frac{\Phi_I^2}{2B_2^4B_3^4a^2}\left(\frac{\Phi_I}{B_2^2B_3^2}\frac{\partial}{\partial\bar{\zeta}^1}(B_2^2B_3^2) + \frac{B_2^2}{B_1^2B_3^2}\Phi_2\frac{\partial}{\partial\zeta^2}(B_3^2) + \frac{B_3^2}{B_1^2B_2^2}\Phi_{s_3}\frac{\partial}{\partial\zeta^3}(B_2^2)\right)\\
&-\frac{\Phi_2^2}{2B_1^4B_3^4a^2}\left(\frac{B_1^2}{B_2^2B_3^2}\Phi_I\frac{\partial}{\partial\bar{\zeta}^1}(B_3^2) + \frac{\Phi_2}{B_1^2B_3^2}\frac{\partial}{\partial\zeta^2}(B_1^2B_3^2) + \frac{B_3^2}{B_1^2B_2^2}\Phi_{s_3}\frac{\partial}{\partial\zeta^3}(B_1^2)\right)
\end{aligned}$$

$$-\frac{\Phi_3^2}{2B_1^4B_2^4a^2}\left(\frac{B_1^2}{B_2^2B_3^2}\Phi_I\frac{\partial}{\partial\bar{\zeta}^1}(B_2^2)+\frac{B_2^2}{B_1^2B_3^2}\Phi_2\frac{\partial}{\partial\zeta^2}(B_1^2)+\frac{\Phi_{s_3}}{B_1^2B_2^2}\frac{\partial}{\partial\zeta^3}(B_1^2B_2^2)\right)$$

where δ_1, δ_2 and δ_3 are the cell dimensions in the $\bar{\zeta}^1$, ζ^2 and ζ^3 directions respectively, and where for the Nth iteration

$$(\Phi_I)_{l,m,n}\simeq(\Phi_{s_I})_{l,m,n}+\frac{\phi_{l+1,m,n}^{(N-1)}-\phi_{l-1,m,n}^{(N)}}{2\delta_1}$$

$$(\phi_{II})_{l,m,n}\simeq(\Phi_{2_{II}})_{l,m,n}+\frac{\phi_{l+1,m,n}^{(N-1)}-2\phi_{l,m,n}^{(N-1)}+\phi_{l-1,m,n}^{(N)}}{\delta_1^2}$$

$$(\Phi_{I2})_{l,m,n}\simeq(\Phi_{s_{I2}})_{l,m,n}+\frac{\phi_{l+1,m+1,n}^{(N-1)}-\phi_{l+1,m,n}^{(N-1)}-\phi_{l-1,m+1,n}^{(N)}+\phi_{l-1,m-1,n}^{(N)}}{4\delta_1\delta_2}$$

with similar expressions for the other derivatives of the point $(\bar{\zeta}_0^1+l\delta_1,\ m\delta_2,\ n\delta_3)$.

$\phi^{(N)}$ is the value of the (unknown) potential obtained for the preset (Nth) iteration cycle, whilst $\phi^{(N-1)}$ is obtained from the previous cycle.

Note we use the latest value of $\phi_{l,m,n}$ available. As well as reducing computer store, this also tends to increase the rate of convergence of the overall system.

Along the singular lines, the equation of continuity reduces to (11), and so the coefficients become simply (neglecting any symmetry or antisymmetry)

$$d_n=\frac{1}{\delta_3^2},\qquad b_n=\frac{1}{\delta_3^2}$$

$$c_n=-2\left(\frac{1}{\delta_2^2}+\frac{1}{\delta_3^2}\right)$$

$$a_n=-\left(\frac{\phi_{l,m+1,n}+\phi_{l,m-1,n}}{\delta_2^2}\right).$$

With symmetry fully invoked, we take the coordinates in the intervals

$$\bar{\zeta}_0^1\leqslant\bar{\zeta}^1\leqslant K'\quad\text{as}\quad 0\leqslant l\leqslant l_m$$
$$0\leqslant\zeta^2\leqslant K\quad\text{as}\quad 0\leqslant m\leqslant m_m$$
$$0\leqslant\zeta^3\leqslant K'\quad\text{as}\quad 0\leqslant n\leqslant n_m$$

i.e.

$$\delta_1=(K'-\bar{\zeta}_0^1)/l_m$$
$$\delta_2=K/m_m$$
$$\delta_3=K'/n_m.$$

Using the body surface boundary condition (5), using reflection, we obtain

$$\phi_{-1,m,n}=\phi_{1,m,n}+2\delta_1\Phi_{s_I}$$

where $(\bar{\zeta}_0^1-\delta_1,\ m\delta_2,\ n\delta_3)$ is a point inside the body.

Symmetry arguments give the following:

for $\Phi_\infty=x$:

$$\phi_{l,-1,n}=\phi_{l,1,n}$$
$$\phi_{l,m_m+1,n}=\phi_{l,m_m-1,n}$$
$$\phi_{l,m,-1}=-\phi_{l,m,1}$$
$$\phi_{l,m,n_m+1}=\phi_{l,m,n_m-1}.$$

for $\Phi_\infty = y$:

$$\phi_{l,-1,n} = \phi_{l,1,n}$$
$$\phi_{l,m_m+1,n} = -\phi_{l,m_m-1,n}$$
$$\phi_{l,m,-1} = \phi_{l,m,1}$$
$$\phi_{l,m,n_m+1} = \phi_{l,m,n_m-1}.$$

The matrix equation (B-1) is now of block tridiagonal form, viz:

$$\begin{bmatrix} c_0 & b_0 & & 0 \\ d_1 & c_1 & b_1 & \\ 0 & d_2 & c_2 & b_2 \\ \cdots & \cdots & \cdots & \cdots \\ 0 & d_{n_m-1} & c_{n_m-1} & b_{n_m-1} \\ & & d_{n_m} & c_{n_m} \end{bmatrix} = \begin{bmatrix} a_0 \\ a_1 \\ a_2 \\ \cdots \\ a_{n_m-1} \\ a_{n_m} \end{bmatrix}$$

Note that because of the symmetry of the problem we can set

$$d_0 = 0$$
$$b_{n_m} = 0.$$

TABLE 1

Variation of Local Mach Number Along $y = 0$, with Mesh Size for $\Phi_\infty = x$, $M_\infty = 0{\cdot}95$, $\sigma = 0{\cdot}04$, $\bar{\zeta}_0^1 = 0{\cdot}10$

$\bar{x}$ \ Point distribution	$6\times21\times10$	$10\times11\times10$	$10\times21\times6$	$10\times21\times10$
0	0·9635	0·9636	0·9623	0·9636
0·0909	0·9635	0·9636	0·9624	0·9636
0·1919	0·9634	0·9635	0·9625	0·9635
0·2929	0·9634	0·9635	0·9626	0·9635
0·3939	0·9633	0·9634	0·9627	0·9634
0·4949	0·9631	0·9633	0·9627	0·9633
0·5960	0·9629	0·9631	0·9627	0·9631
0·6970	0·9625	0·9628	0·9625	0·9628
0·7980	0·9616	0·9620	0·9623	0·9620
0·8990	0·9582	0·9591	0·9596	0·9591
0·9596	0·9468	0·9498	0·9520	0·9499
0·9697	0·9407	0·9448	0·9479	0·9449
0·9798	0·9301	0·9347	0·9374	0·9350
0·9899	0·9142	0·9111	0·9142	0·9112
1·0	0	0	0	0

Ratio of axes 1 : 0·2010 : 0·0200

$$\bar{x} = \frac{x}{[1+(\zeta^1)^2]^{\frac{1}{2}}}$$

TABLE 2

Variation of Local Mach Number Along $x = 0$, with Mesh Size for $\Phi_\infty = y$, $M_\infty = 0{\cdot}80$, $\sigma = 0{\cdot}04$, $\bar{\zeta}_0^1 = 0{\cdot}10$

$\bar{y}$ \ Point distribution	$20\times11\times20$	$15\times15\times20$	$20\times21\times15$	$20\times15\times20$	$15\times21\times20$	$20\times21\times20$
0	0·9613	0·9592	0·9618	0·9616	0·9593	0·9617
0·0909	0·9607	0·9587	0·9613	0·9611	0·9589	0·9613
0·1919	0·9593	0·9573	0·9599	0·9597	0·9574	0·9599
0·2929	0·9569	0·9547	0·9575	0·9572	0·9549	0·9574
0·3939	0·9529	0·9509	0·9537	0·9534	0·9511	0·9537
0·4949	0·9475	0·9454	0·9483	0·9480	0·9456	0·9483
0·5960	0·9400	0·9375	0·9406	0·9403	0·9378	0·9406
0·6970	0·9286	0·9260	0·9292	0·9290	0·9262	0·9292
0·7980	0·9096	0·9067	0·9102	0·9097	0·9071	0·9103
0·8990	0·8691	0·8696	0·8704	0·8711	0·8689	0·8704
0·9596	0·7931	0·8065	0·8025	0·7997	0·8097	0·8026
0·9697	0·7580	0·7860	0·7792	0·7766	0·7894	0·7792
0·9798	0·7165	0·7347	0·7313	0·7238	0·7438	0·7313
0·9899	0·6075	0·6401	0·6369	0·6287	0·6503	0·6370
1·0	0	0	0	0	0	0

Ratio of axes 1 : 0·2010 : 0·200

$$\bar{y} = \frac{y}{[\sigma+(\zeta_0^1)^2]^{\frac{1}{2}}}$$

TABLE 3

Mach Number Distribution on Surface of Ellipsoid $\Phi_\infty = x, \sigma = 0{\cdot}04, M_\infty = 0{\cdot}95, \bar{\zeta}_0^1 = 0{\cdot}10$
$10 \times 21 \times 10$ Mesh

$\bar{x}$ \ $\bar{y}$	0	0·1111	0·2222	0·3333	0·6667	1·0
0	0·9636	0·9636	0·9636	0·9636	0·9636	0·9636
0·0909	0·9636	0·9636	0·9636	0·9636	0·9636	
0·1919	0·9635	0·9635	0·9635	0·9635	0·9635	
0·2929	0·9635	0·9635	0·9635	0·9635	0·9635	
0·3939	0·9634	0·9634	0·9634	0·9634	0·9635	
0·4949	0·9633	0·9633	0·9633	0·9633	0·9634	
0·5960	0·9631	0·9631	0·9632	0·9632	0·9633	
0·6970	0·9628	0·9628	0·9628	0·9629	0·9631	
0·7980	0·9620	0·9620	0·9622	0·9624	0·9628	
0·8990	0·9591	0·9593	0·9600	0·9606	0·9620	
0·9596	0·9499	0·9511	0·9538	0·9563	0·9602	
0·9697	0·9449	0·9468	0·9507	0·9545	0·9593	
0·9798	0·9350	0·9390	0·9458	0·9517	0·9577	
0·9899	0·9112	0·9217	0·9361	0·9454	0·9543	
1·0	0	0·4157	0·6789	0·8105	0·9343	

Ratio of axes 1 : 0·2010 : 0·0200

$$\bar{y} = \frac{y}{[\sigma + (\zeta^1)^2]^{\frac{1}{2}}}, \qquad \bar{x} = \frac{x}{[1 + (\zeta^1)^2]^{\frac{1}{2}}[1 - \bar{y}^2]^{\frac{1}{2}}} \qquad (\bar{y} < 1)$$

$$= 0 \qquad (\bar{y} = 1)$$

TABLE 4

Mach Number Distribution on Surface of Ellipsoid $\Phi_\infty = y, \sigma = 0{\cdot}04, M_\infty = 0{\cdot}80, \bar{\zeta}_0^1 = 0{\cdot}10$
$20 \times 21 \times 20$ Mesh

$\bar{y}$ \ $\bar{x}$	0	0·1111	0·2222	0·3333	0·6667	1·0
0	0·9617	0·9617	0·9617	0·9618	0·9623	0·9680
0·0909	0·9613	0·9613	0·9613	0·9614	0·9619	
0·1919	0·9599	0·9599	0·9599	0·9600	0·9605	
0·2929	0·9574	0·9574	0·9575	0·9576	0·9582	
0·3939	0·9537	0·9537	0·9537	0·9538	0·9545	
0·4949	0·9483	0·9483	0·9484	0·9485	0·9494	
0·5960	0·9406	0·9406	0·9407	0·9409	0·9420	
0·6970	0·9292	0·9292	0·9293	0·9295	0·9313	
0·7980	0·9103	0·9103	0·9105	0·9108	0·9133	
0·8990	0·8704	0·8705	0·8707	0·8712	0·8750	
0·9596	0·8026	0·8027	0·8031	0·8037	0·8094	
0·9697	0·7792	0·7794	0·7798	0·7806	0·7872	
0·9798	0·7313	0·7315	0·7319	0·7327	0·7397	
0·9899	0·6370	0·6372	0·6377	0·6386	0·6466	
1·0	0	0·0193	0·0393	0·0609	0·1522	

Ratio of axes 1 : 0·2010 : 0·0200

$$\bar{x} = \frac{x}{[1 + (\zeta_0^1)^2]^{\frac{1}{2}}}, \qquad \bar{y} = \frac{y}{[\sigma + (\zeta_0^1)^2]^{\frac{1}{2}}[1 - \bar{x}^2]^{\frac{1}{2}}} \qquad (\bar{x} < 1)$$

$$= 0 \qquad (\bar{x} = 1)$$

TABLE 5

Mach Number Distribution on Surface of Ellipsoid $\Phi_\infty = x$, $\sigma = 0{\cdot}04$, $M_\infty = 0{\cdot}80$, $\bar{\zeta}_0^1 = 0{\cdot}10$
$10 \times 21 \times 10$ Mesh

$\bar{x}$ \ $\bar{y}$	0	0·1111	0·2222	0·3333	0·6667	1·0
0	0·8086	0·8086	0·8086	0·8086	0·8086	0·8086
0·0909	0·8086	0·8086	0·8086	0·8086	0·8086	
0·1919	0·8087	0·8087	0·8087	0·8087	0·8086	
0·2929	0·8087	0·8087	0·8087	0·8087	0·8086	
0·3939	0·8087	0·8087	0·8087	0·8087	0·8086	
0·4949	0·8087	0·8087	0·8087	0·8087	0·8086	
0·5960	0·8087	0·8087	0·8087	0·8087	0·8086	
0·6970	0·8086	0·8086	0·8086	0·8086	0·8086	
0·7980	0·8083	0·8084	0·8084	0·8084	0·8084	
0·8990	0·8073	0·8073	0·8075	0·8077	0·8079	
0·9596	0·8035	0·8039	0·8047	0·8055	0·8066	
0·9697	0·8014	0·8020	0·8032	0·8045	0·8060	
0·9798	0·7968	0·7983	0·8007	0·8027	0·8047	
0·9899	0·7856	0·7897	0·7949	0·7982	0·8020	
1·0	0	0·3628	0·5830	0·6886	0·7859	

Ratio of axes 1 : 0·2010 : 0·0200

$$\bar{y} = \frac{y}{[\sigma + (\zeta^1)^2]^{\frac{1}{2}}}, \qquad \bar{x} = \frac{x}{[1 + (\zeta_0^1)^2]^{\frac{1}{2}}[1 - \bar{y}^2]^{\frac{1}{2}}} \qquad (\bar{y} < 1)$$

$$= 0 \qquad (\bar{y} = 1)$$

TABLE 6

Mach Number Distribution on Surface of Ellipsoid $\Phi_\infty = y$, $\sigma = 0{\cdot}04$, $M_\infty = 0{\cdot}70$, $\bar{\zeta}_0^1 = 0{\cdot}10$
$20 \times 21 \times 20$ Mesh

$\bar{y}$ \ $\bar{x}$	0	0·1111	0·2222	0·3333	0·6667	1·0
0	0·8075	0·8075	0·8075	0·8075	0·8076	0·8099
0·0909	0·8073	0·8073	0·8073	0·8074	0·8074	
0·1919	0·8069	0·8069	0·8069	0·8069	0·8071	
0·2929	0·8061	0·8062	0·8062	0·8062	0·8063	
0·3939	0·8050	0·8050	0·8050	0·8050	0·8051	
0·4949	0·8031	0·8031	0·8031	0·8031	0·8034	
0·5960	0·8003	0·8003	0·8003	0·8003	0·8006	
0·6970	0·7956	0·7956	0·7957	0·7957	0·7961	
0·7980	0·7868	0·7868	0·7869	0·7870	0·7876	
0·8990	0·7645	0·7645	0·7646	0·7647	0·7659	
0·9596	0·7172	0·7173	0·7175	0·7177	0·7201	
0·9697	0·6994	0·6995	0·6997	0·7000	0·7032	
0·9798	0·6602	0·6603	0·6605	0·6609	0·6643	
0·9899	0·5799	0·5800	0·5803	0·5808	0·5851	
1·0	0	0.0169	0·0344	0·0532	0·1329	

Ratio of axes 1 : 0·2010 : 0·0206

$$\bar{x} = \frac{x}{[1 + (\zeta_0^1)^2]^{\frac{1}{2}}}, \qquad \bar{y} = \frac{y}{[\sigma + (\zeta^1)^2]^{\frac{1}{2}}[1 - \bar{x}^2]^{\frac{1}{2}}} \qquad (\bar{x} < 1)$$

$$= 0 \qquad (\bar{x} = 1)$$

TABLE 7

Mach Number Distribution on Surface of Ellipsoid $\Phi_\infty = x$, $\sigma = 0{\cdot}50$, $M_\infty = 0{\cdot}90$, $\bar{\zeta}_0^1 = 0{\cdot}10$
$10 \times 21 \times 10$ Mesh

$\bar{x}$ \ $\bar{y}$	0	0·1111	0·2222	0·3333	0·6667	1·0
0	0·9896	0·9896	0·9896	0·9896	0·9896	0·9894
0·0909	0·9892	0·9892	0·9892	0·9892	0·9891	
0·1919	0·9882	0·9882	0·9883	0·9884	0·9886	
0·2929	0·9866	0·9866	0·9868	0·9868	0·9875	
0·3939	0·9841	0·9842	0·9843	0·9845	0·9859	
0·4949	0·9807	0·9808	0·9810	0·9814	0·9838	
0·5960	0·9759	0·9760	0·9764	0·9771	0·9807	
0·6970	0·9691	0·9688	0·9694	0·9705	0·9766	
0·7980	0·9546	0·9554	0·9569	0·9591	0·9694	
0·8990	0·9248	0·9261	0·9296	0·9343	0·9555	
0·9596	0·8727	0·8758	0·8827	0·8925	0·9285	
0·9697	0·8546	0·8579	0·8650	0·8757	0·9177	
0·9798	0·8267	0·8313	0·8397	0·8489	0·9002	
0·9899	0·7596	0·7658	0·7791	0·7935	0·8578	
1·0	0	0·1318	0·2612	0·3870	0·7247	

Ratio of axes 1 : 0·7089 : 0·0707

$$\bar{y} = \frac{y}{[\sigma + (\zeta_0^1)^2]^{\frac{1}{2}}}, \qquad \bar{x} = \frac{x}{[1 + (\zeta_0^1)^2]^{\frac{1}{2}}[1 - \bar{y}^2]^{\frac{1}{2}}} \qquad (\bar{y} < 1)$$

$$= 0 \qquad (\bar{y} = 1)$$

TABLE 8

Mach Number Distribution on Surface of Ellipsoid $\Phi_\infty n = y$, $\sigma = 0{\cdot}50$, $M_\infty = 0{\cdot}70$, $\bar{\zeta}_0^1 = 0{\cdot}10$
$20 \times 21 \times 20$ Mesh

$\bar{y}$ \ $\bar{x}$	0	0·1111	0·2222	0·3333	0·6667	1·0
0	0·7851	0·7851	0·7851	0·7851	0·7854	0·7859
0·0909	0·7850	0·7850	0·7850	0·7850	0·7853	
0·1919	0·7846	0·7846	0·7847	0·7847	0·7850	
0·2929	0·7840	0·7840	0·7840	0·7841	0·7844	
0·3939	0·7830	0·7830	0·7831	0·7831	0·7836	
0·4949	0·7815	0·7815	0·7816	0·7817	0·7823	
0·5960	0·7792	0·7792	0·7792	0·7794	0·7803	
0·6970	0·7753	0·7753	0·7755	0·7756	0·7770	
0·7980	0·7677	0·7678	0·7681	0·7686	0·7710	
0·8990	0·7481	0·7482	0·7486	0·7492	0·7548	
0·9596	0·7019	0·7025	0·7040	0·7066	0·7152	
0·9697	0·6775	0·6780	0·6794	0·6818	0·6996	
0·9798	0·6447	0·6456	0·6481	0·6524	0·6701	
0·9899	0·5532	0·5545	0·5583	0·5647	0·6085	
1·0	0	0·0573	0·1159	0·1771	0·3968	

Ratio of axes 1 : 0·7089 : 0·0707

$$\bar{x} = \frac{x}{[1 + (\zeta_0^1)^2]^{\frac{1}{2}}}, \qquad \bar{y} = \frac{y}{[\sigma + (\zeta_0^1)^2]^{\frac{1}{2}}[1 - \bar{x}^2]^{\frac{1}{2}}} \qquad (\bar{x} < 1)$$

$$= 0 \qquad (\bar{x} = 1)$$

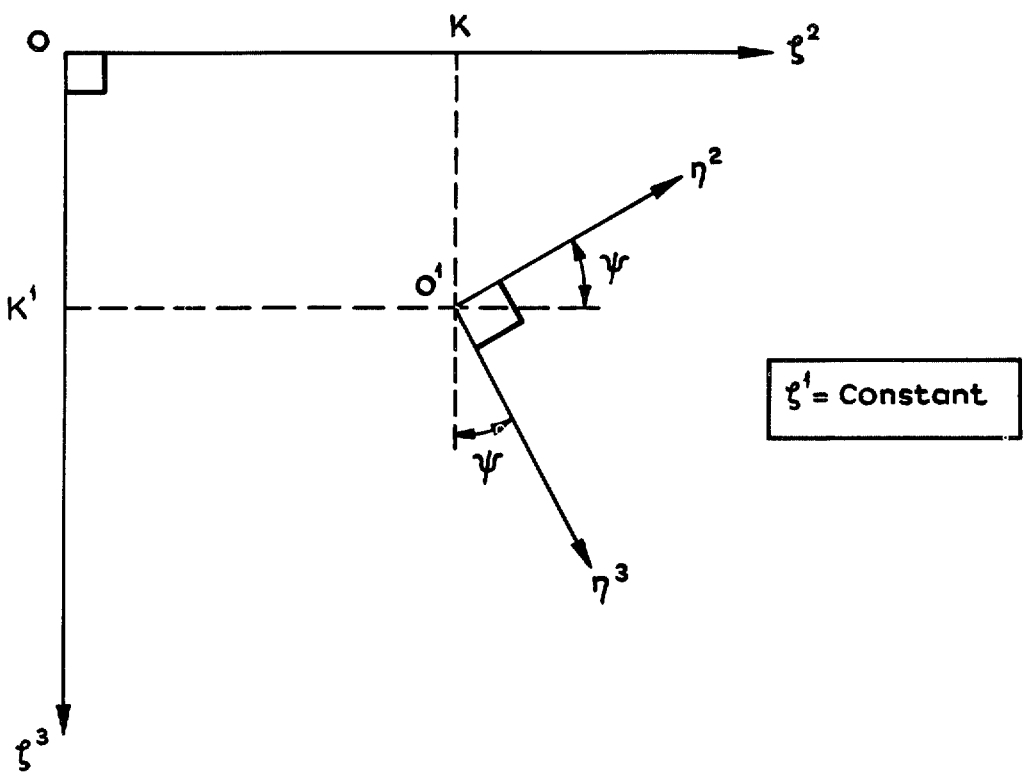

FIG. 1. Rotated coordinate scheme.

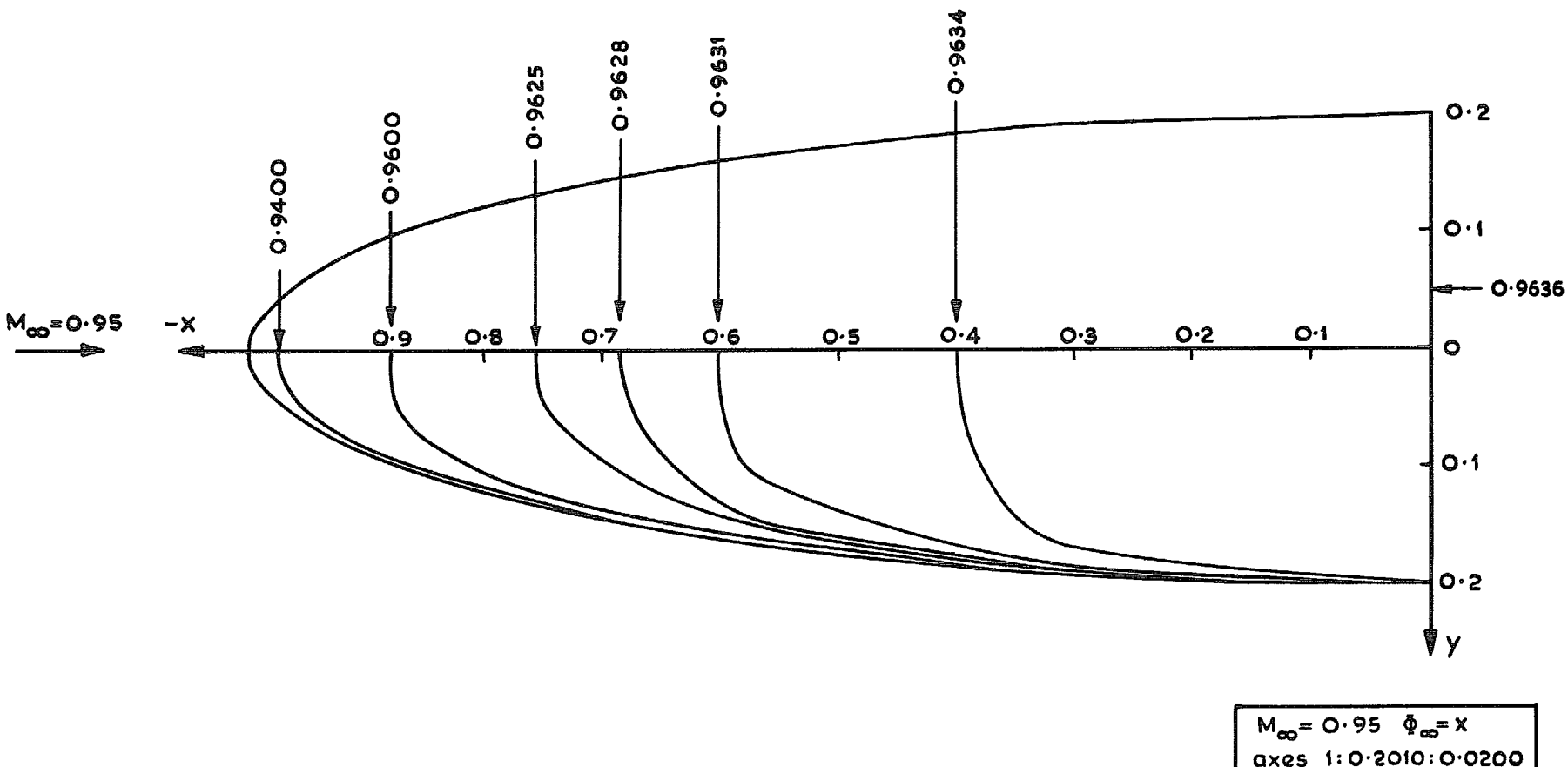

FIG. 2. Lines of constant Mach number.

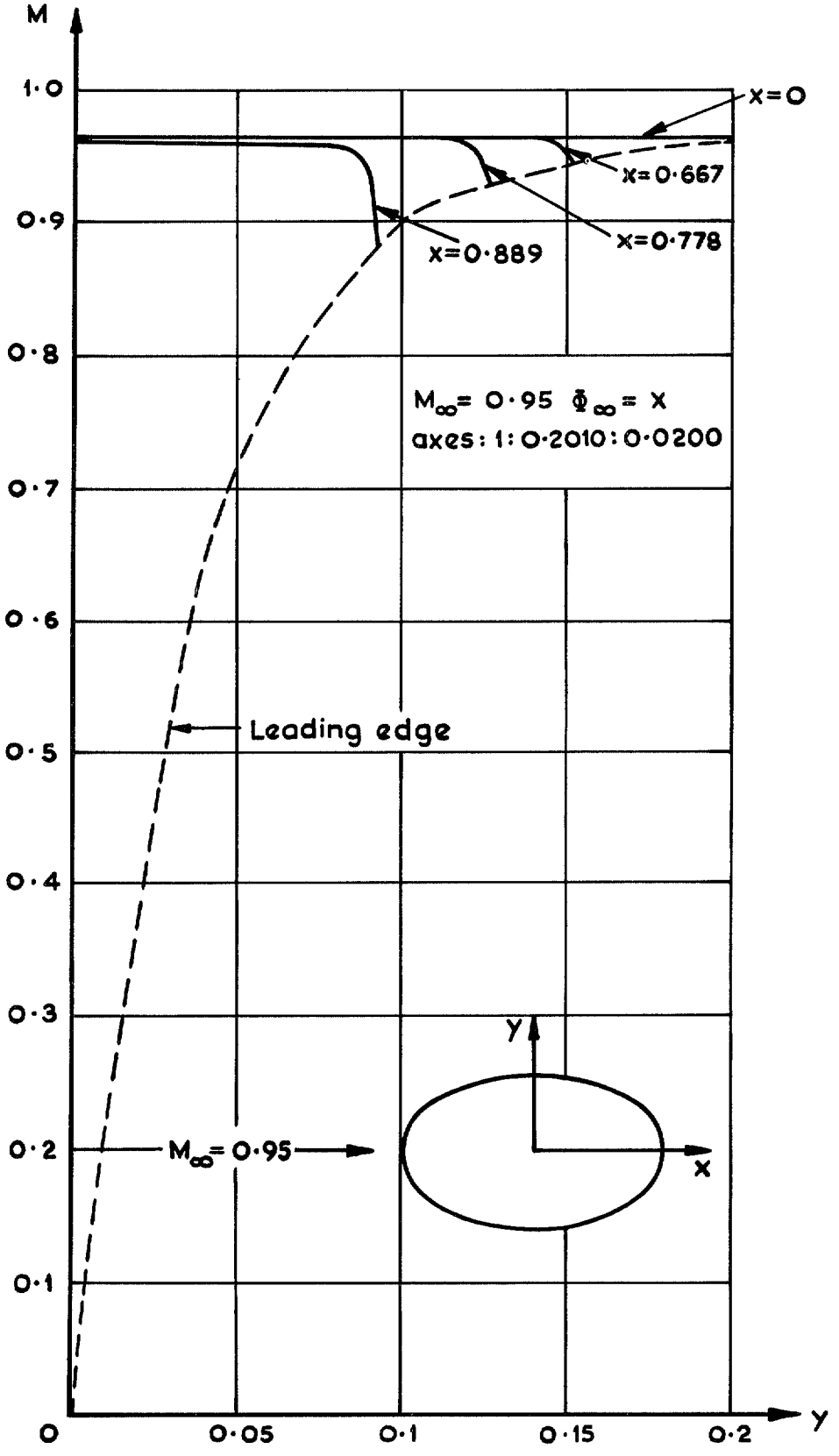

FIG. 3. Mach number distribution on surface of ellipsoid.

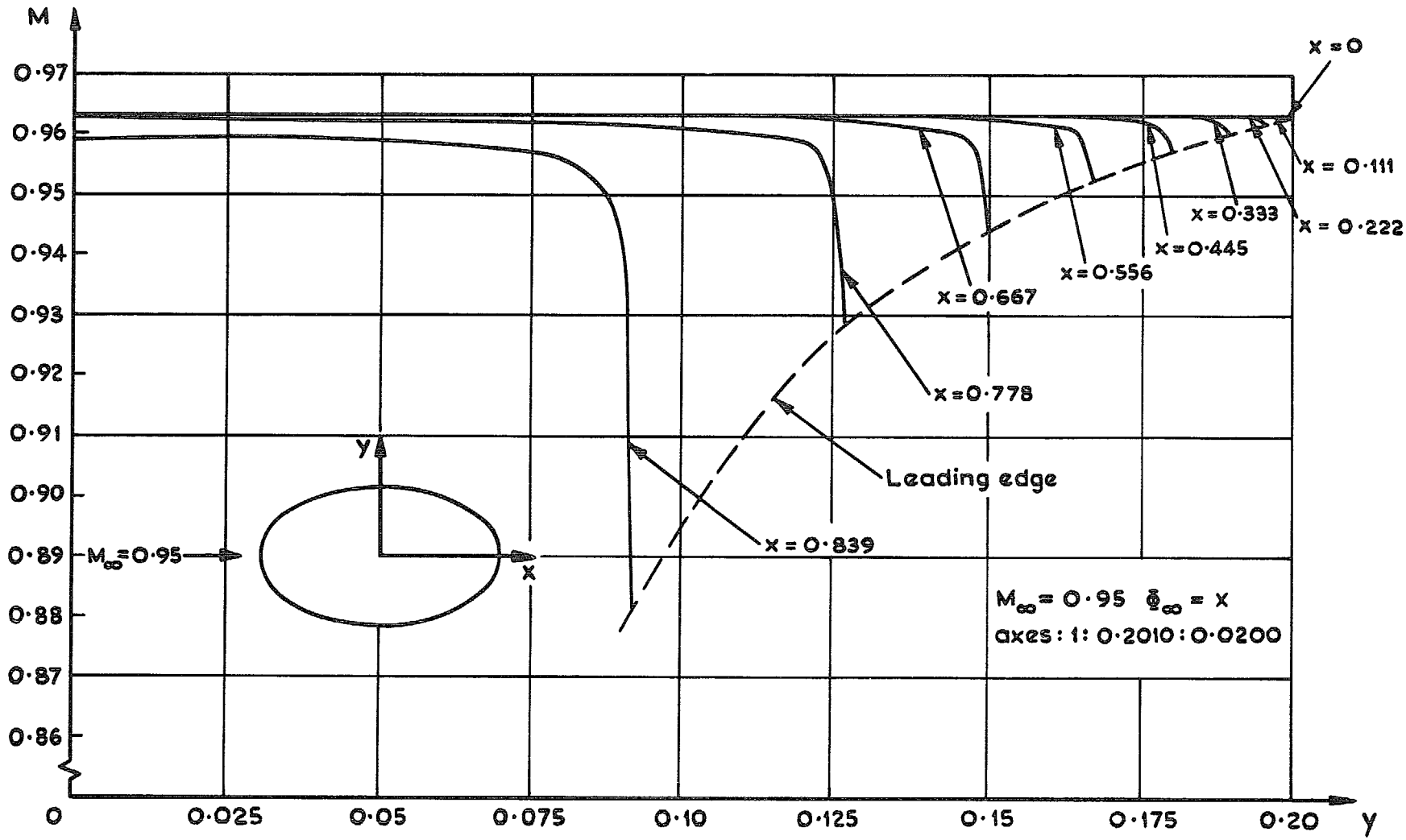

FIG. 4. Mach number on surface of ellipsoid.

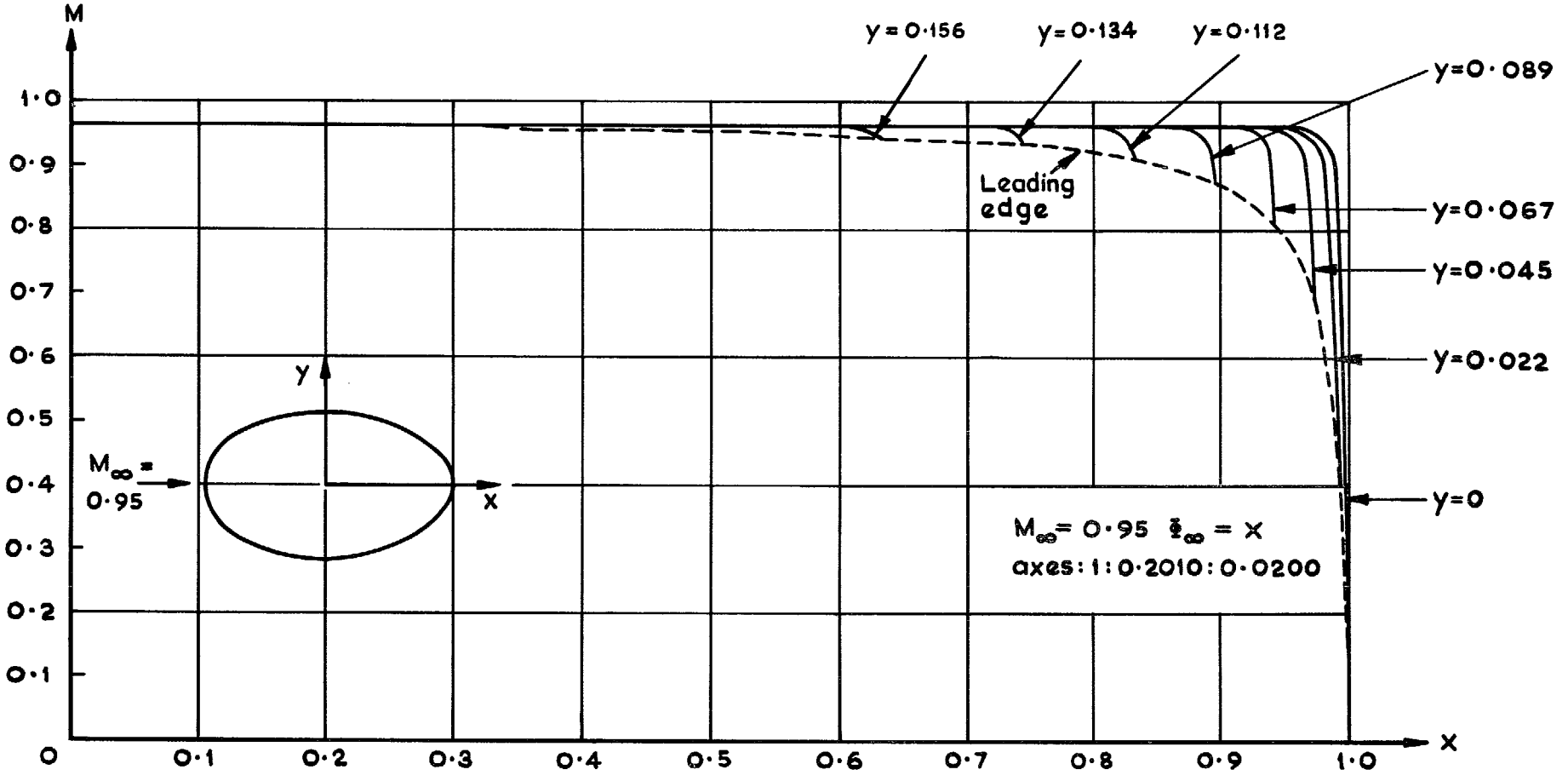

FIG. 5. Mach number distribution on surface of ellipsoid.

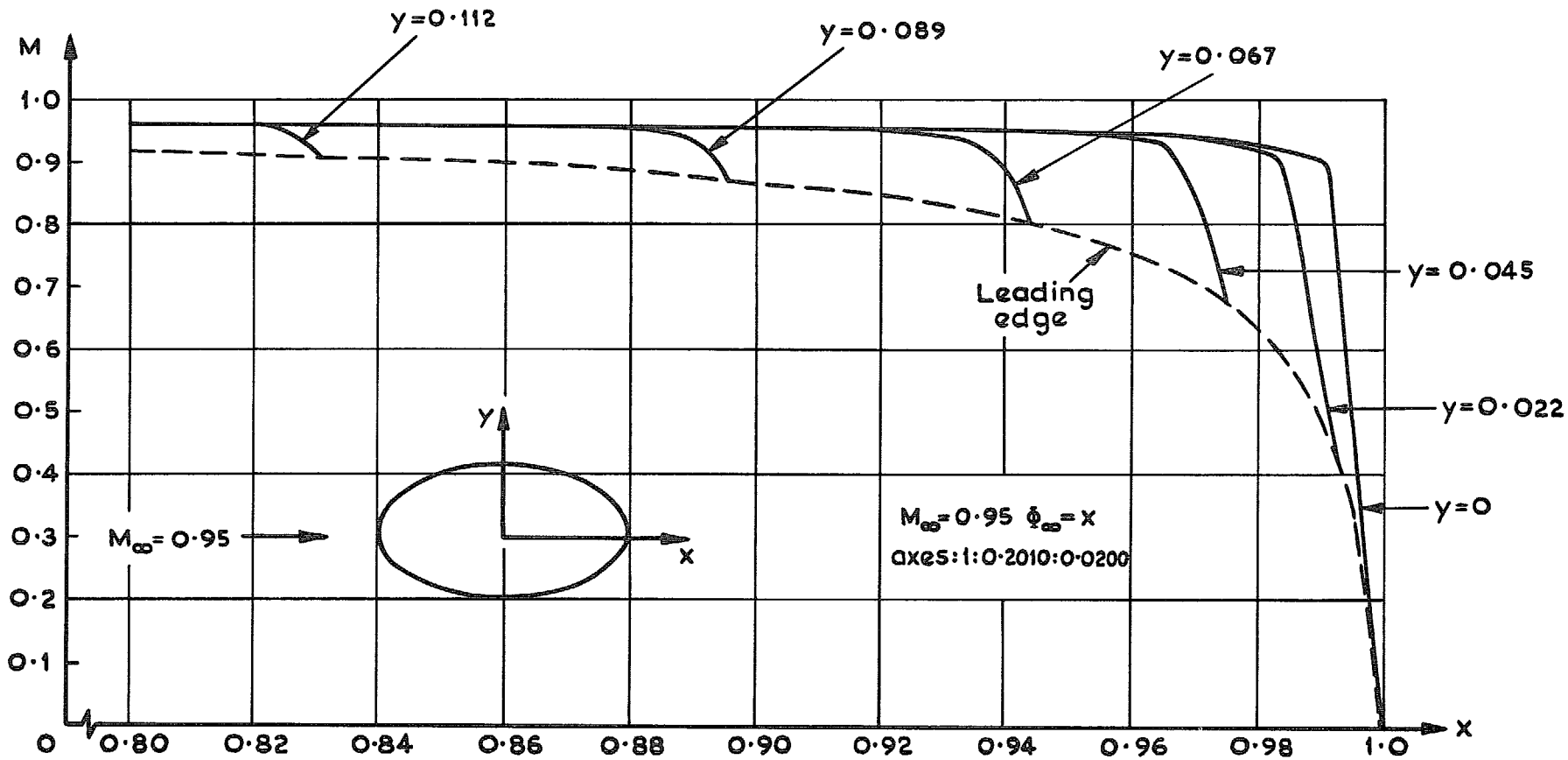

FIG. 6. Mach number distribution on surface of ellipsoid.

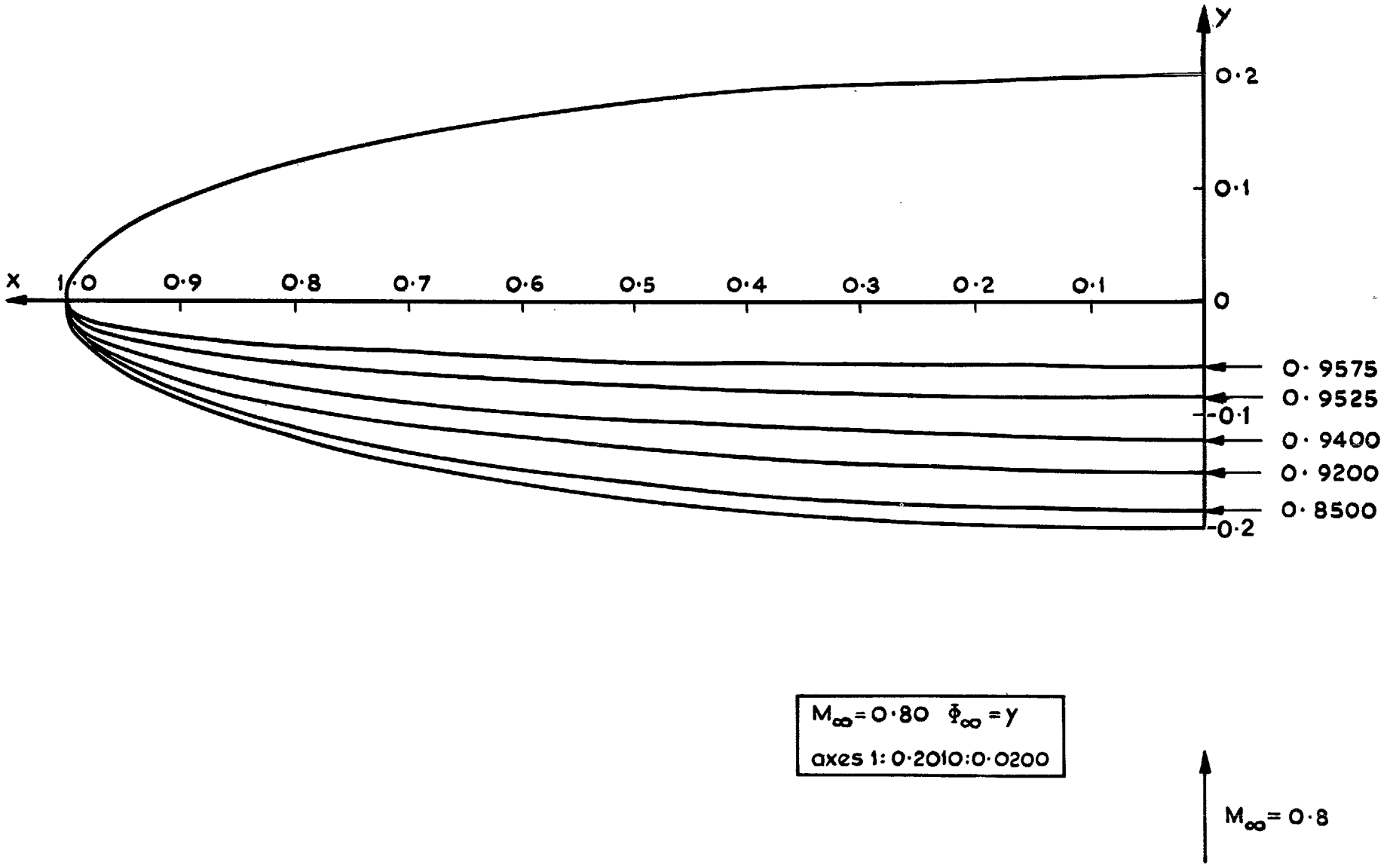

FIG. 7. Lines of constant Mach number.

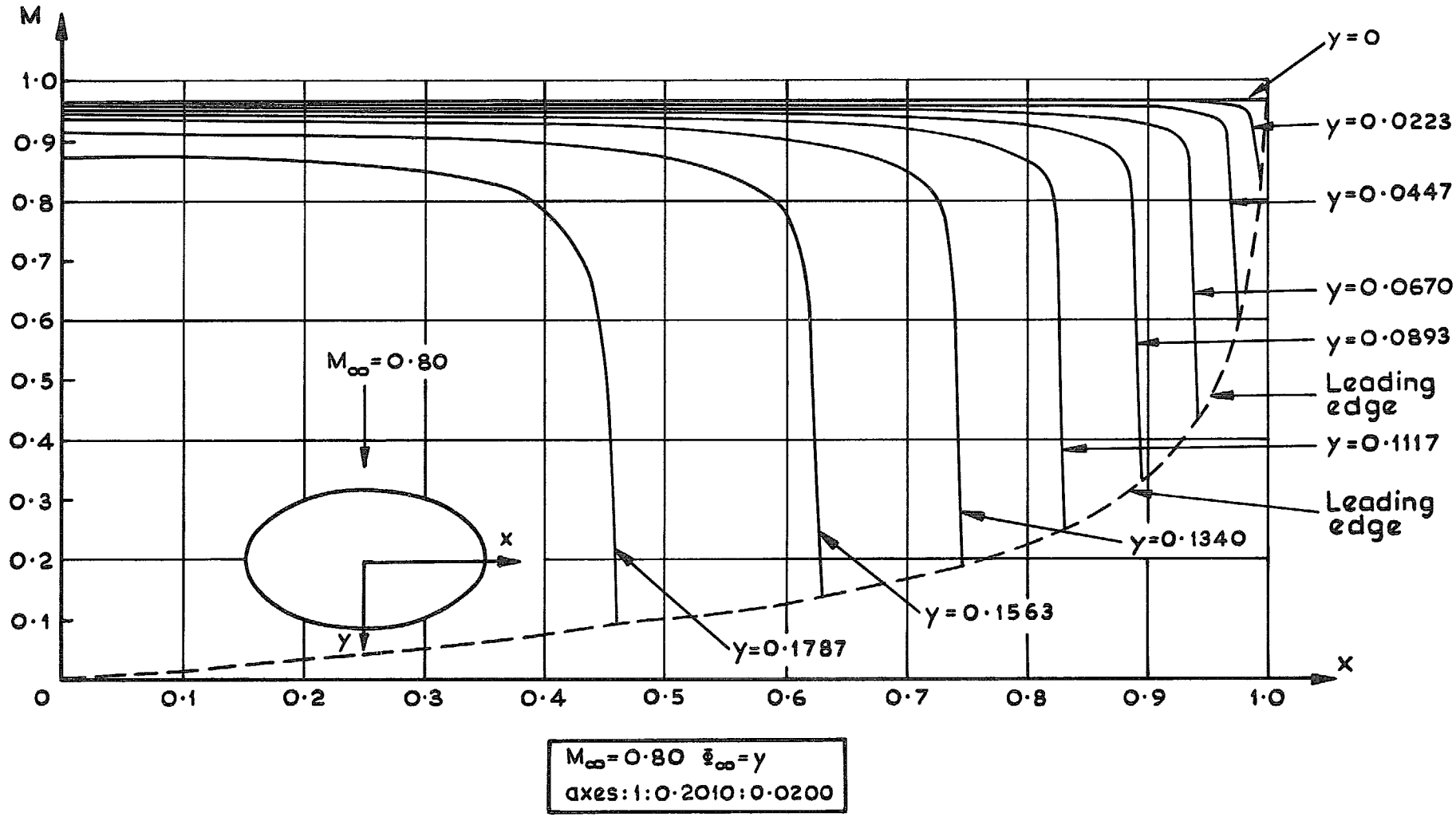

FIG. 8. Mach number distribution on surface of ellipsoid.

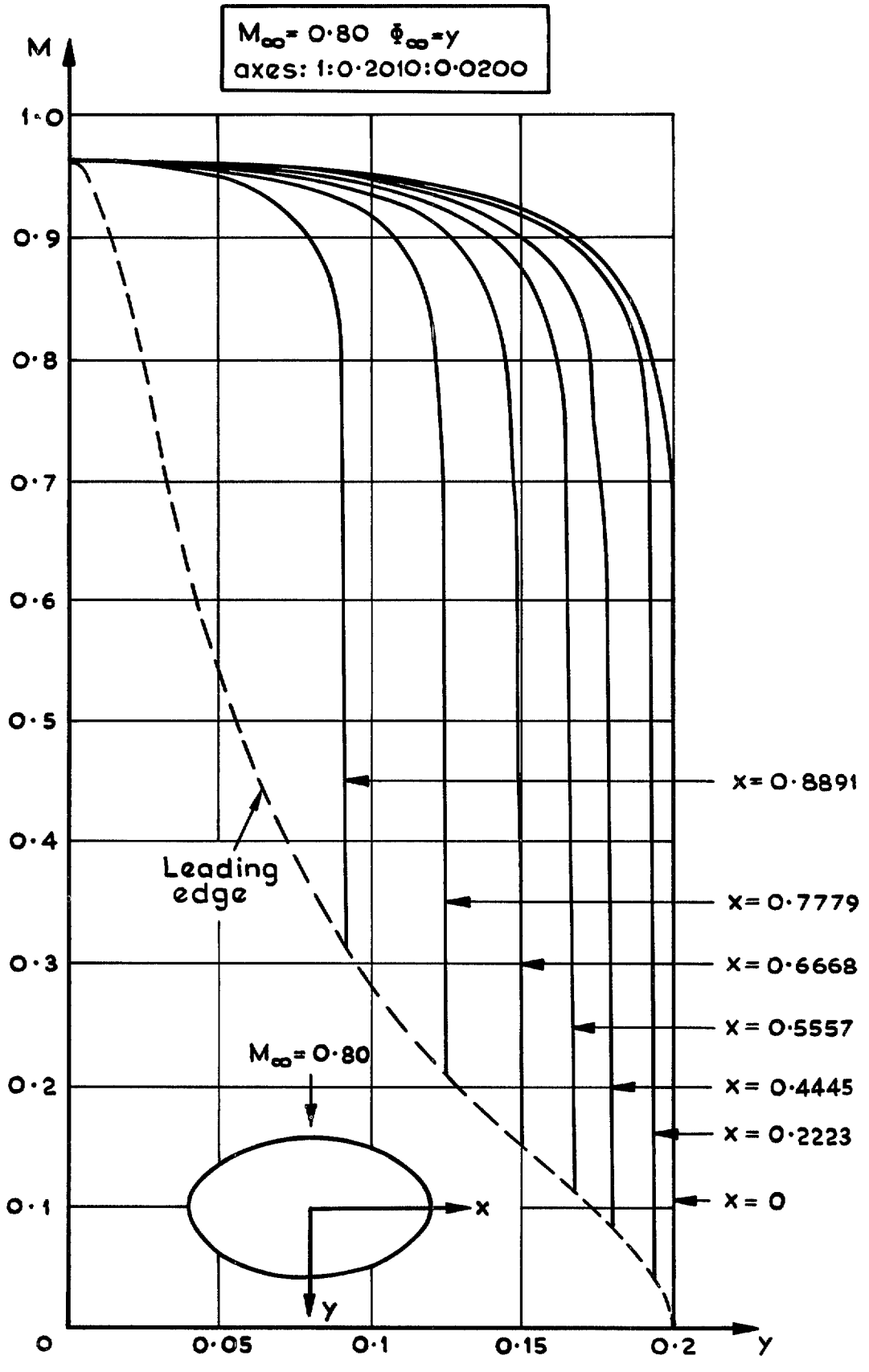

FIG. 9. Mach number distribution on surface of ellipsoid.

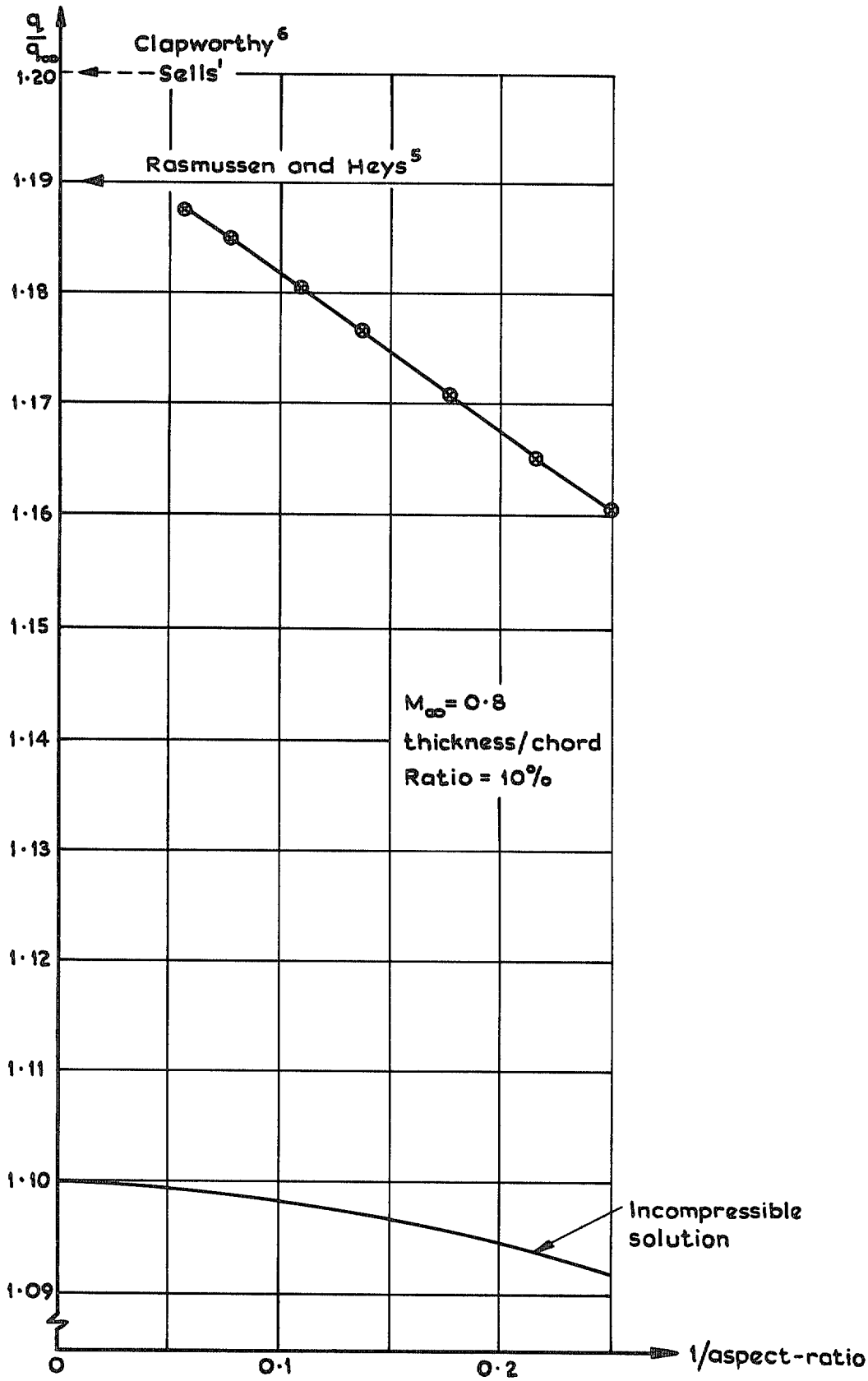

FIG. 10. Variation of normalized flow velocity at centre of upper (and lower) surface of ellipsoid with 1/aspect-ratio.

Printed in England for Her Majesty's Stationery Office by J. W. Arrowsmith Ltd., Bristol BS3 2NT
Dd. 290278 K.5. 2/77.

HER MAJESTY'S STATIONERY OFFICE

Government Bookshops

49 High Holborn, London WC1V 6HB
13a Castle Street, Edinburgh EH2 3AR
41 The Hayes, Cardiff CF1 1JW
Brazennose Street, Manchester M60 8AS
Southey House, Wine Street, Bristol BS1 2BQ
258 Broad Street, Birmingham B1 2HE
80 Chichester Street, Belfast BT1 4JY

Government Publications are also available through booksellers

R. & M. No. 3795

ISBN 0 11 470966 1